Altered Interneuron Development in the Cerebral Cortex of the *Flathead* Mutant

Matthew R. Sarkisian, Mikhail Frenkel, Weiwei Li, Justin A. Oborski and Joseph J. LoTurco

Department of Physiology and Neurobiology, University of Connecticut, Storrs, CT, USA

One approach to defining mechanisms essential to neocortical development is to analyze the phenotype of novel spontaneous mutations that dramatically affect the generation and differentiation of different neocortical neurons. Previously we have shown that there is a large decrease in the total number of cortical neurons in the *flathead* mutant rat, and in this paper we show that the *flathead* (*fh/fh*) mutation causes an even larger decrease in the number of interneurons. The decrease in relative interneuron number is different in different cortical lamina and for different interneuron subtypes. Specifically, the percentage of GABA and calretinin-positive cells in upper layers of somatosensory cortex is not appreciably decreased in homozygous mutants, while other interneuron subtypes in somatosensory cortex and all GABA-positive interneuron types in entorhinal cortex are decreased. In addition, the soma and dendritic arbors of interneurons in *flathead* are greatly hypertrophied, while those of pyramidal neurons are not. Furthermore, we found that at embryonic day 14, *flathead* mutants display high levels of cell death throughout both the neocortical and ganglionic eminence (GE) proliferative zones with a larger increase in cell death in the GE than in the neocortical VZ. In addition, we provide evidence that there is widespread cytokinesis failure resulting in binucleate pyramidal cells and interneurons, and the number of binucleate interneurons is greater than the number of binucleate pyramidal neurons. Together, these results demonstrate that the *fh* mutation causes dramatic alterations in interneuron development, and suggest that the *flathead* mutation causes differential cytokinesis failure and cell death in different types of neocortical progenitors.

Introduction

Normal cortical function is dependent upon the balanced development of two major neuron types: pyramidal cells and non-pyramidal cells. Non-pyramidal neurons primarily contain the neurotransmitter γ-amino butyric acid (GABA), and make up 15–30% of all cortical neurons (Parnavelas *et al*., 1977; Hendry *et al*., 1987; Meinecke and Peters, 1987) while the, primarily glutamatergic, pyramidal neurons constitute the remainder. GABAergic interneuron subtypes are further classified by different morphologies, expression of different calcium-binding proteins and distinct electrophysiological properties (McCormick *et al*., 1985; Kawaguchi and Kubota, 1993) [for review see (DeFelipe, 1997; Gupta *et al*., 2000)]. The distribution and differentiation of interneuron subtypes is believed to determine area- and lamina-specific physiologies, and disruptions in interneuron number have been related to epilepsy (Ribak *et al*., 1982; Ferrer *et al*., 1994; Spreafico *et al*., 1998) and schizophrenia (Benes *et al*.,1991; Kalus *et al*., 1997). The mechanisms that determine the appropriate number of interneurons relative to pyramidal neurons or the genesis and differentiation of different interneuron types are not well understood.

Recent cellular and genetic evidence suggests that most interneurons of the cerebral cortex do not arise from the neocortical VZ of the dorsal telencephalon, but rather from the MGE (Anderson *et al*., 1999, 2001; Lavdas *et al*., 1999; Sussel *et al*., 1999; Wichterle *et al*, 1999) [for review see (Parnavelas, 2000; Parnavelas *et al*., 2000)]. A stream of tangentially migrating cells from the ganglionic eminence enters the neocortex (De Carlos *et al*., 1996; Anderson *et al*., 1997; Tamamaki *et al*., 1997), and mice lacking homeobox genes, *Dlx1* and *Dlx2*, have a reduced ganglionic eminence and have far fewer GABAergic cells at birth (Anderson *et al*., 1997). While together these data suggest that most inhibitory interneurons stem from the ganglionic eminence and most likely the MGE (Lavdas *et al*., 1999; Anderson *et al*., 1999, 2001), it still remains unclear as to whether other embryonic factors ultimately interact to regulate the appropriate laminar composition of interneurons and pyramidal neurons in neocortex.

Flathead is a recently described autosomal recessive mutation in rat located on the long arm of chromosome 12, 2cM telomeric to *Nos*-1 (Cogswell *et al*., 1998). The central nervous system (CNS)-specific phenotype has been recently described, and includes microencephaly, increased cell death throughout the developing nervous system and spontaneous seizures (Sarkisian *et al*., 1999; Roberts *et al*., 2000). A striking feature of the *flathead* cerebral cortex is its 40% reduction in size at birth. The neocortex of *fh/fh* mutants is approximately half its normal thickness and layers II/III are dramatically reduced while deeper layers (IV–VI) appear less affected. The effects on specific laminae are associated with a temporal pattern of late embryonic cell death. A reduction in upper layer thickness corresponds with an ~20-fold increase in cell death in the VZ at embryonic day (E) 18 compared to *wt*, as well as a continued increase in cell death in the cortical plate at birth (Roberts *et al*., 2000). In contrast, large amounts of cell death were not observed in the VZ before E16 or beyond postnatal day (P) 8 (Roberts *et al*, 2000). However, at the time of the initial study by Roberts *et al.* (Roberts *et al*., 2000), a genotypic marker was not available to identify unambiguously *fh/fh* mutants earlier than E18, and therefore conclusively determining the pattern of cell death in confirmed *fh/fh*'s earlier than E18 was not possible. In this study, we have used a genetic marker <1 cM to the *fh* mutation to genotype *fh/fh* mutants and study cellular defects during the period of interneuron generation (~E13–16).

While we are in the initial stages of identifying the molecular nature of the *fh* mutation, a recent report describing mice that lack Citron-kinase (Citron-K) reveals striking similarities to the *flathead* phenotype (Di Cunto *et al*., 2000). Remarkably, these similarities include a 40% reduction in the size of the cerebral cortex at birth, anatomical abnormalities in cerebellum and hippocampus, an ~50% reduction in neocortical thickness including laminar changes similar to *flathead*, early onset epilepsy, severe ataxia and early postnatal death. In addition, both the *flathead* rat (this study) and Citron-K mutant mice have

severe deficits in interneuron generation and alterations in cytokinesis leading to many binucleated neurons. Moreover, Citron-K is highly expressed throughout proliferating areas of the CNS prior to birth (Di Cunto *et al.*, 2000). In addition, the genetic location of the *fh* mutation in rat is homologous to the region of human chromosome 12 which contains the *Citron* gene. Here we report that the *fh* mutation results in a widespread decrease in the relative numbers of interneurons and in a selective increase in interneuron growth. We also show evidence of cell death throughout the neocortical-VZ and MGE, cytokinesis abnormalities in both precursor cells in MGE, and pyramidal and non-pyramidal cells throughout postnatal neocortex. These observations suggest the *fh/fh* gene causes a defect in the genesis of CNS precursors due to a failed cytokinesis process that subsequently alters the number and size of neocortical interneurons.

Materials and Methods

Animals

A total of 124 (n = 56 *fh/fh*'s, n = 68 littermates) rats, ranging in age from E14 to P21, were used in this study. Mutant animals were from either of two colonies: the original Wistar rat colony in which the *fh* mutation spontaneously occurred (WUC1), and a colony generated from an F1 interstrain cross (Lewis × WUC1), allowing for the genotyping of animals (see below) (Cogswell *et al.*, 1998). All animal protocols were in accordance with the University of Connecticut IACUC guidelines.

Materials

Primary antibodies used in this study were rabbit anti-GABA (Sigma, St Louis, MO), mouse anti-parvalbumin (Chemicon, Temecula, CA), mouse anti-calbindin-D28k (Sigma), mouse anti-NeuN (Chemicon), mouse anti-rat brain pyramidal cells (SWant, Bellinzola, Switzerland) and mouse anti-calretinin (Chemicon). Secondary antibodies included biotinylated goat anti-rabbit and goat anti-mouse (Vector Laboratories, Burlingame, CA), Texas red dye-conjugated goat anti-mouse and goat anti-rabbit (Jackson Immunoresearch, West Grove, PA), and fluorescein-conjugated goat anti-rabbit (Molecular Probes, Eugene, OR). Other materials used were 4 μM 4,6-diamidino-2-phenylindole (DAPI; Sigma), 1,1′-dioctodecyl-3,3,3′,3′-tetramethylindocarbocyanine (DiI) (Molecular Probes), normal goat serum (NGS) (Vector), avidin and biotin (Vector), Cytoseal mounting medium (Stephens Scientific, Kalamazoo, MI), Vectashield fluorescence mounting media (Vector), Prolong™ anti-fade mounting media (Molecular Probes), and diaminobenzidine (Vector). Genomic DNA was purified using a kit purchased from Qiagen (Valencia, CA). The MapPair™ primers, D12rat80, were purchased from Research Genetics (Huntsville, AL).

Immunocytochemistry

Standard immunocytochemical procedures were used for the following primary antibodies: mouse anti-calbindin D28k (CAL) (1:1000), mouse anti-calretinin (CR) (1:1000), mouse anti-parvalbumin (PARV) (1:1000), rabbit anti-GABA (1:10,000), mouse anti-NeuN (1:1000), and mouse anti-rat brain pyramidal cells (1:7500). For BrdU ICC, timed-pregnant heterozygous dams (*+/fh*) received a single i.p. injection of BrdU (Sigma) at 60 mg/kg in saline with 0.007 N NaOH on E14. The litters were perfused with 4% paraformaldehyde at P13. Cryostat sections (10–15 μm) were processed for BrdU ICC with anti-BrdU (1:1; Amersham, Arlington Heights, IL). Sections were treated with 2 N HCl and neutralized with borate buffer. After incubation in anti-BrdU at 4°C overnight, sections were processed with the indirect avidin–biotin horseradish peroxidase technique and visualized with diaminobenzidine.

At P0, several brains were paraffin embedded, sectioned into 4 μm horizontal sections at 40 μm intervals and stained with hematotoxylin and eosin (H&E) with Luxol Fast Blue to determine neuronal density. Brains from several embryos were processed for electron microscopy (EM) and were post-fixed overnight in 2% paraformaldehyde and 0.75% glutaraldehyde in 0.12 M PB. Sections (500 μm) were cut on a vibratome in the coronal plane and small regions of VZ and MGE were subdissected. These sections were post-fixated by osmication in 2% osmium tetroxide in 0.12 M PB and then dehydrated through an ethanol series ending in propylene oxide. The tissues were embedded in an epoxy mixture containing SPI-PON 812 and ALDITE 605. Sections were cut using glass knives at 90 nm, post-stained with uranyl acetate and lead citrate, and viewed on a Phillips 300 microscope at 80 kV. Semithin (1 μm) tissue sections were also prepared for light microscopy and stained with toluidine blue for general cell labeling, detection of mitotic figures and presence of pyknotic nuclei (Martín-Partido *et al.*, 1986).

Regional Determination and Quantification of Cells

Cell counts were obtained from sections of E14, P0 and P14 *fh/fh* mutants and wildtypes (at least two or three *fh/fh* and two or three *wt* rats/group). For P0 and P14 rats, all cell counts were obtained from sections of comparable horizontal planes between *wt* and *fh/fh*. For each stain, five counting boxes were systematically placed across upper and deeper layers (as defined below) of entorhinal (EC) or somatosensory (SS) neocortices, and all labeled cells within each box counted [areas (in μm2) for boxes at P14: NeuN-EC and SS = 11 880, GABA–EC = 11 880, GABA-SS = 51 984, CAL-EC = 11 880, CAL-SS = 51 984, CR-EC = 51 984, CR-SS= 11 880, PARV-EC = 11 880, PARV-SS = 51 984; areas (in μm^2) of boxes at P0: GABA and H&E-EC = 1600, GABA and H&E-SS = 5400]. While the area of the NeuN counting box was smaller than the boxes used for GABA, CAL and CR, consistent neuronal densities were routinely obtained as boxes were systematically placed across the counting region of interest, suggesting that cell density was constant over each counting region. The percentage of GABA+, CAL+, CR+ and PARV+ interneurons was determined for SS and EC regions of cerebral cortex by dividing the density of each interneuron cell type in each region by the density of H&E or NeuN+ cells in each region.

For EC, we used the following histological landmarks to identify upper (II/III) or deeper (primarily VI) layers for NeuN, GABA, CR, CAL and PARV+ cells. For NeuN, we defined upper layers by placing counting boxes centered between the internal border of layer I and lamina dissecans. Boxes were first placed at the anterior part of lamina dissecans with subsequent boxes added posteriorly. Similarly, deeper layers were operationally defined by placing counting boxes centered between lamina dissecans and white matter. For GABA, boxes were similarly placed for upper layers along the internal border of layer I and above white matter for deeper layers. For CR, boxes were placed in upper layers, centered between layer I and lamina dissecans (identified by the thick band of immunoreactivity – see Fig. 2*A*). For CAL, boxes were placed in upper layers, centered within a white, non-fiberous band such that the bottom edge of the box did not extend below lamina dissecans. For PARV, boxes were placed in upper layers, and were centered within the thick fibrous band characteristic of layer II/III immunoreactivity in EC (Wouterlood *et al.*, 1995).

For SS, a line 300 μm anterior to the tip of CA3 of hippocampus was extended radially toward neocortex in *fh/fh* and *wt* rats. This served as an indicator of where to begin placing counting boxes with subsequent boxes added systematically towards the anterior. To place appropriately sized counting boxes within upper (II/III) and deeper (primarily VI) layers of SS, we referred to CAL and cytochrome oxidase staining as landmarks for determining lamination patterns of layers II/III and IV respectively (Roberts *et al.*, 2000). For NeuN, GABA and CR, we defined upper layers by placing boxes such that the upper edges of the counting boxes were adjacent to the internal border of layer I. For the same stains, we defined deeper layers of SS by placing counting boxes such that the bottom edge of the box was slightly (~10–20 μm) above white matter. For CAL, we counted deeper layers by placing boxes slightly above white matter (Sánchez *et al.*, 1992). For PARV, upper layers were defined by placing counting boxes centered between layer I and the darkly stained puncta of layer IV, a defining feature of PARV immunoreactivity in SS, while in deeper layers, boxes were placed slightly above white matter and beneath the thick band of layer IV labeling (Sánchez *et al.*, 1992).

We found that in upper layers of EC, NeuN density was significantly increased in *fh/fh* compared to *wt* [mean *wt* = 23 ± 6, *fh/fh* = 30 ± 4; $F(1,22) = 10.77$, P 0.01] while neuronal density was decreased in deeper layers of *fh/fh* rats compared to *wt* [mean *wt* = 51 ± 10, mean *fh/fh* = 40 ± 8; $F(1,22) = 19.45$, $P < 0.001$]. In upper layers of SS cortex, we found that neuronal density was decreased in *fh/fh* compared to *wt* [mean *wt* = 57 ±

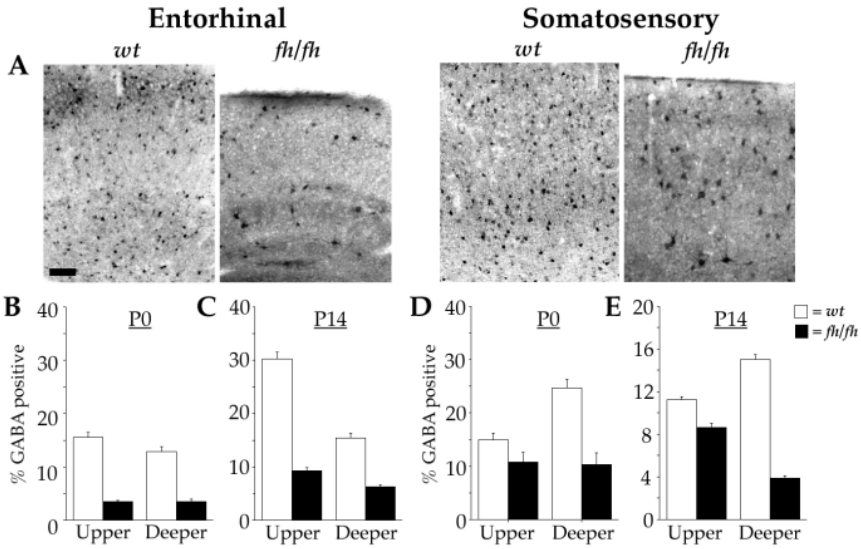

Figure 1. Reduction in the percentage of GABA+ neurons in entorhinal (EC) and somatosensory (SS) cortex. (*A*) Expression patterns of GABA+ neurons in *wt* and *fh/fh* rats at P14 in EC (left panels) and SS (right panels) cortex. (*C*,*E*) Quantitative analysis of the percentage of GABA+ neurons in upper (II/III) and deeper (primarily VI) layers of EC (*C*) and SS (*E*) at P14 in *wt* (open bars) and *fh/fh* (closed bars). While all layers in both regions showed significant reductions in the density of GABA+ neurons, the magnitude of the decrease in upper layers of SS is not as great as in other regions. (*B*,*D*) Quantification of the percentage of GABA+ neurons in EC (*B*) and SS (*D*) cortex at P0 shows a similar pattern in reduction to that observed at P14. Scale bar = 50 μm.

10, *fh/fh* = 33 ± 5; $F(1,30) = 71.30$, $P < 0.001$]. Neuronal density was also decreased in deeper layers of SS cortex in *fh/fh* rats [mean *wt* = 48 ± 7, *fh/fh* = 42 ± 4; $F(1,30) = 9.55$; $P < 0.01$]. At P0 interneuron densities were placed over a grand mean of H&E-stained cells. Neuronal density at P0 was not significantly different in upper or deeper layers of EC (for upper: mean *wt* = 18 ± 1, *fh/fh* = 18 ± 2; $P > 0.05$; for deeper: mean *wt* = 22 ± 1, *fh/fh* = 23 ± 2; $P > 0.05$).

At E14, we quantified the percentage of pyknotic nuclei within semithin sections of MGE and neocortical VZ. Pyknotic nuclei were defined as darkly stained, punctate nuclei (see Fig. 5*A*) and those nuclei that were fragmented were counted as one nucleus. Images of MGE and VZ sections were imported into Adobe Photoshop 5.0 and the total number of nuclei and pyknotic nuclei were counted within 50 μm zones beginning and extending 400–600 μm away from the ventricular surface. To calculate the percentage of dead cells within each 50 μm zone, we divided the total number of pyknotic nuclei by the total number of nuclei within each 50 μm area counted.

Analysis of Cell Morphology

Images of all labeled cells were acquired on a Nikon Eclipse E400 microscope using a Spot digital camera. Soma area, nuclear area, number of primary dendrites and average dendritic width were determined from digitized images. Primary dendrites were considered processes originating from the soma, and dendritic widths were measured at a constant distance of 20 μm from the cell body. All measurements were performed by an observer blind to the experimental groups.

Retrograde DiI Labeling

To compare morphologies of projecting pyramidal cells between *fh/fh* and *wt* rats, P15 rats (n = 2 *fh/fh* and 2 *wt*) were perfused with 1 × PBS followed by 4% paraformaldehyde and then post-fixed overnight at 4°C. Crystals of DiI were then placed into the right cerebral hemisphere using a glass micropipette. The brains were then placed into PBS containing 1 mM sodium azide and incubated at 37°C for 8–12 weeks. Coronal sections (50 μm) were taken and labeled pyramidal cells (primarily those in layers II/III and V) were analyzed in both the ipsi- and contralateral hemisphere.

PCR-based Genotyping of +/+, +/fh and fh/fh Mutants

Genomic DNA was purified from either spleens (P14) or bodies (E14 and E15) using a Qiagen QIAamp® DNA Mini Kit. We performed polymerase chain reaction (PCR) with the MapPair™ marker D12Rat80, which is <1 cM from the *fh* mutation (Cogswell *et al.*, 1998). This allowed us to genotype wildtype (+/+), heterozygous (+/*fh*) or mutant (*fh/fh*) rats. Because +/+ and +/*fh* animals exhibit similar phenotypes and appear behaviorally normal, we have collectively referred to both of these genotypes as *wt* phenotype for purposes of immunohistological comparisons.

Statistical Analyses

Comparisons of neuronal densities and morphological measurements across ages were evaluated using ANOVA. Comparisons of interneuron densities and soma sizes between different neocortical regions were made using a three-factor ANOVA with repeated measures. A P-value <0.05 was considered significant.

Results

Reduction in the Density of GABA+ Neurons in Cerebral Cortex

In order to determine the relative number of inhibitory interneurons to total neurons in the cerebral cortex of *flathead* and wildtype rats, we used immunocytochemistry for GABA and the neuronal nuclear antigen, NeuN. Figure 1*A* shows examples of GABA immunoreactivity in EC and SS for *wt* and *fh/fh* rats at P14. As shown in Figure 1*C*,*E*, in both areas, and in all layers, the percentage of GABA+ neurons was reduced. In upper layers of EC, ~30% of neurons in *wt* compared to 9% of neurons in *fh/fh* were GABA+, while in deeper layers of EC ~15% of neurons in *wt* compared to 6% of neurons in *fh/fh* were GABA+ [for upper: $F(1,53) = 308.05$, $P < 0.001$; for deeper: $F(1,53) = 104.23$, $P < 0.001$]. In deeper layers of SS ~15% of neurons in *wt* compared to 4% in *fh/fh* were GABA+. In contrast, in upper layers of SS there was only a slight decrease in the percentage of GABA+ neurons: ~11% of neurons in *wt* compared to 9% of neurons in *fh/fh* [for upper: $F(1,35) = 28.99$, $P < 0.01$, for deeper: $F(1,35) = 543.46$, $P < 0.001$]. Therefore, the *flathead* mutation causes a widespread decrease in the relative number of inhibitory interneurons. Moreover, the decrease in interneuron loss suggests death is

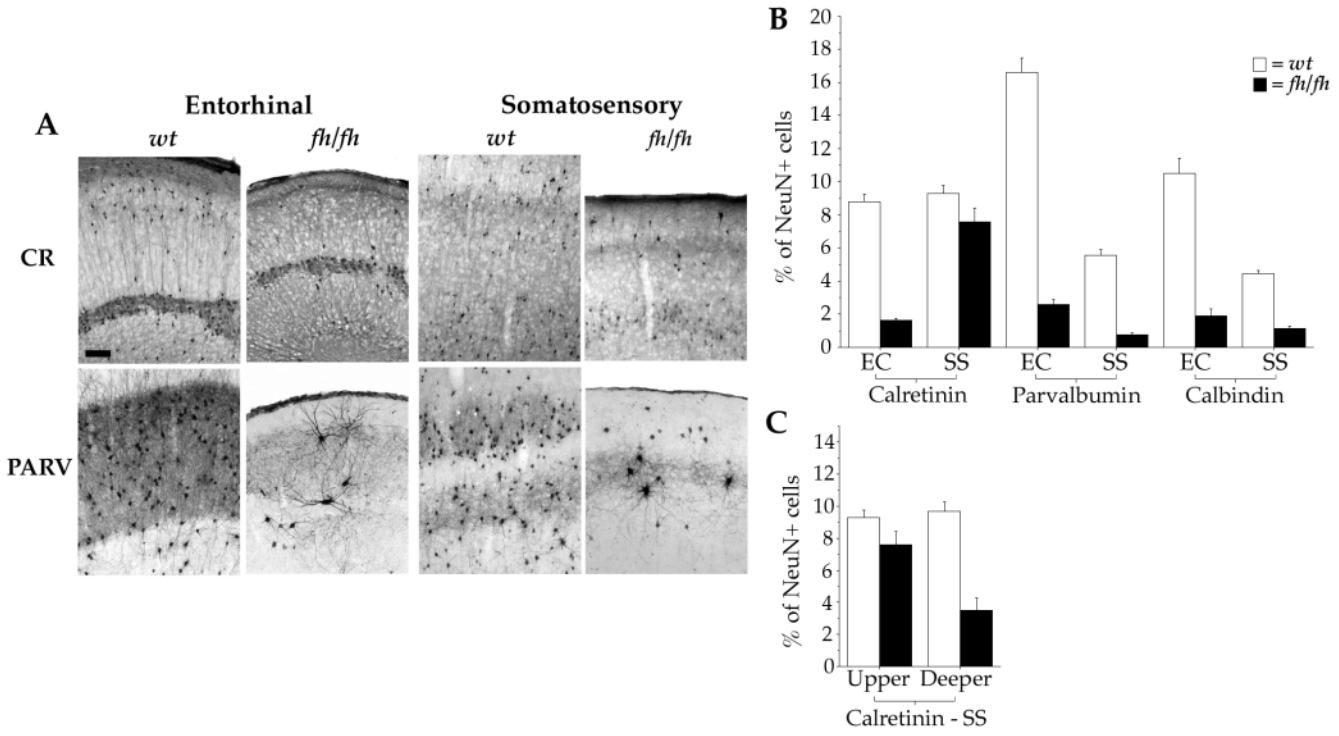

Figure 2. Reductions in three interneuron subtypes in *fh/fh*. (*A*) Expression patterns of cells positive for CR (upper panels) and PARV (lower panels) in EC and SS at P14. (*B*) Comparison of the percentages of CR+, PARV+ and CAL+ neurons in EC and SS at P14 in *wt* (open bars) and *fh/fh* (closed bars). All percentages represent cell type density in upper layers of EC and SS except for CAL-SS, where the percentages represent density in deeper layers. Percentage reductions in CR, PARV and CAL in *fh/fh* ranged from 2- to 6-fold in the different cortical regions; however, there was no significant reductions in upper layers of SS cortex for CR. (*C*) Percentages of CR+ neurons in upper and deeper layers of SS cortex. In contrast to upper layers, there is a decrease of CR+ cells in deeper layers of SS cortex. Scale bar = 50 μm.

significantly different in different cortical regions and layers (three-factor ANOVA; $F = 68.3$, $P < 0.001$).

Since *flathead* has seizures beginning the end of the first postnatal week, and it is possible that the reduction in interneurons is secondary to seizures, we determined the percentage of GABA+ neurons in EC and SS on the day of birth, ~1 week before seizures begin (Sarkisian *et al*., 1999). As shown in Figure 1*B*, in upper layers of EC at P0 ~16% of neurons in *wt* compared to 3% in *fh/fh* were GABA+, while in deeper layers ~13% of neurons in *wt* compared to 4% in *fh/fh* were GABA+ [for upper: $F(1,53) = 178.82$, $P < 0.001$; for deeper: $F(1,53) = 107.54$, $P < 0.001$]. The reduction in inhibitory interneurons was of similar magnitude in EC before seizure activity becomes apparent either behaviorally or electrophysiologically (Sarkisian *et al*., 1999). In P0 SS cortex, a similar pattern of reduction compared to P14 was also observed. As shown in Figure 1*D*, in upper layers of SS ~15% of neurons in *wt* compared to 11% in *fh/fh* were GABA+, while in deeper layers ~25% of neurons in *wt* compared to 10% in *fh/fh* were GABA+ [for upper: $P > 0.05$; for deeper: $F(1,8) = 24.21$, $P < 0.01$]. Therefore, the reduction in interneurons appears to be a prenatal effect and is likely to result from the failed genesis, migration or increased death of interneuron precursors.

Reduction of Interneuron Subpopulations

The calcium-binding proteins CR, PARV and CAL are specifically expressed in populations of GABA+ interneurons in the cerebral cortex (Celio, 1990; Kawaguchi and Kubota, 1993; Alcántara *et al*, 1996; Cauli *et al*., 1997) [for review see (DeFelipe 1997)]. To determine if the *flathead* mutation differentially affects subpopulations of interneurons in different cortical areas and layers, we determined the percentage of neurons positive for each of the three calcium binding proteins in upper and deeper layers of SS and EC cortices.

Figure 2*A* shows examples of CR and PARV immunoreactivity in EC and SS for both *wt* and *fh/fh* rats. As shown in Figure 2*B*, PARV+ and CAL+ cells are decreased in both regions of EC and SS. In upper layers of EC, ~11% of neurons in *wt* compared to 2% in *fh/fh* were CAL+, while ~17% of neurons in *wt* compared to 3% in *fh/fh* were PARV+ [for upper of EC: CAL; $F(1,25) = 53.75$, $P < 0.001$; PARV; $F(1,28) = 199.74$, $P < 0.001$]. In upper layers of SS, 6% of neurons in *wt* compared to 1% in *fh/fh* were PARV+ and in deeper layers of SS, ~5% of neurons in *wt* compared to 1% in *fh/fh* were PARV+, while ~5% of neurons in *wt* compared to 1% in *fh/fh* were CAL+ [for upper of SS: PARV – $F(1,38) = 262.94$, $P < 0.001$; for deeper: CAL – $F(1,46) = 196.66$, $P < 0.001$; PARV – $F(1,37) = 473.70$, $P < 0.001$]. In contrast, CR+ cells are decreased in upper layers of EC [~9% of cells in *wt* compared to 2% in *fh/fh*: $F(1,22) = 296.23$, $P < 0.001$], but not in upper layers of SS cortex (~9% of neurons in *wt* compared to 8% in *fh/fh*) (Fig. 2*B*,*C*). However, as shown in Figure 2*C*, the percentage of CR+ neurons is decreased in deeper layers of SS cortex [~10% of neurons in *wt* compared to 4% in *fh/fh*: $F(1,23) = 37.21$, $P < 0.001$]. Therefore, the *flathead* mutation results in a widespread reduction in interneuron subtypes but largely spares CR+ interneurons in upper layers of SS cortex.

Hypertrophy of Interneurons

While interneurons are greatly decreased in number, the sizes of individual interneurons are markedly enhanced in *fh/fh*. Figure 3*A* shows examples of CR+, PARV+ and CAL+ interneurons in *wt* and *fh/fh* neocortex. Figure 3*B* shows a quantification of soma

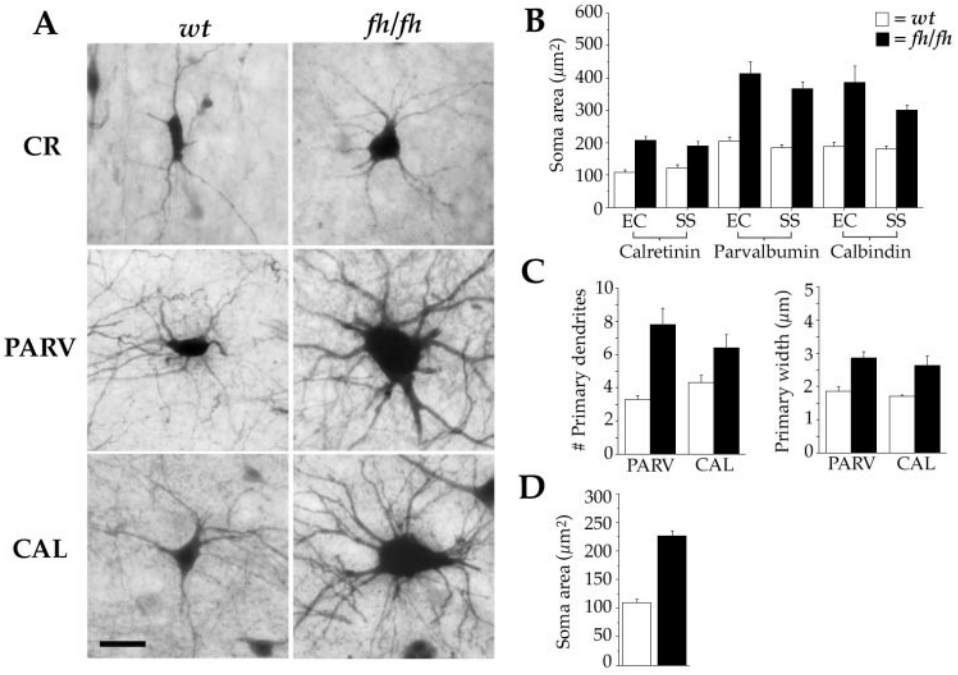

Figure 3. Interneurons are larger in *fh/fh*. (*A*) Examples of CR+, PARV+ and CAL+ neurons in *wt* (left column) and *fh/fh* (right column) rats at P14. (*B*) Quantification of soma areas of CR, PARV and CAL neurons in EC and SS at P14 in *wt* (open bars) and *fh/fh* (closed bars). Soma sizes were significantly increased in all cortical areas for all cell types. (*C*) Quantification of the number of primary dendrites and primary dendritic width from PARV+ and CAL+ neurons from both *wt* and *fh/fh* rats. For both PARV and CAL, there were approximately twice as many primary dendrites and an increase in the thickness of dendritic processes. (*D*) Quantification of soma sizes of GABA-immunoreactive neurons at P0 shows that the increase in soma size is present by birth. Scale bar = 50 μm.

Table 1
Morphology and distribution of CR+, CAL+ and PARV+ cells in EC and SS cortex

Interneuron subtype		Soma area (μm²)		No. of primary dendrites		Primary width (μm)			% of neurons in EC		% of neurons in SS	
		wt	*fh/fh*	*wt*	*fh/fh*	*wt*	*fh/fh*		*wt*	*fh/fh*	*wt*	*fh/fh*,
CR	EC:	110 ± 24	207 ± 45***	ND		ND		Upper:	9	2***	9	8 (NS)
	SS:	122 ± 36	191 ± 37***					Deeper:	ND		10	4***
CAL	EC:	189 ± 46	386 ± 195***	4.3 ± 1.3	6.4 ± 2.5*	1.7 ± 0.1	2.6 ± 0.9**	Upper:	11	2***	ND	
	SS:	181 ± 38	301 ± 63***					Deeper:	ND		5	1***
PARV	EC:	205 ± 45	414 ± 144***	3.3 ± 0.7	7.8 ± 3.1***	1.8 ± 0.5	2.9 ± 0.6***	Upper:	17	3***	6	1***
	SS:	184 ± 41	366 ± 82***					Deeper:	ND		5	1***

Somas of CR+ (n = 15 *wt*, 15 *fh/fh*), CAL+ (n = 15 *wt*, 15 *fh/fh*) and PARV+ (n = 15 *wt*, 15 *fh/fh*) cells are hypertrophied in both EC and SS of P14 *fh/fh* rats. The largest CAL+ (n = 10 *wt*,10 *fh/fh*) and PARV+ (n = 10 *wt*,10 *fh/fh*) cells in *fh/fh* have increases in the number of primary dendrites and a corresponding increase in primary dendritic widths. Also shown for comparison are the percentages of CR+, CAL+ and PARV+ neurons in upper and deeper layers of EC and SS at P14. Percentages in some layers of EC or SS were not determined (ND). *$P < 0.05$, **$P < 0.01$, ***$P < 0.001$; $P > 0.05$ not significant (NS).

size from randomly selected PARV+, CAL+ and CR+ neurons from EC and SS neocortices. For each of these regions we observed general hypertrophy of all three interneuron subtypes (Fig. 3*B* and Table 1). We quantified the number of primary dendrites and the width of primary dendrites of the largest PARV+ and CAL+ cells in *fh/fh* and *wt*. As shown in Figure 3*C* and Table 1, PARV+ cells have more than twice as many primary dendrites and a corresponding increase in primary dendritic width and, similarly, CAL+ cells in *fh/fh* have more primary dendrites and an increase in primary dendritic widths.

To determine if the interneuron hypertrophy was present before seizure onset in early development, we determined whether GABA+ cells were hypertrophied at P0. As shown in Figure 3*D*, we found that somas of GABA+ neurons taken from across neocortex at P0 were larger in *fh/fh* (n = 33 cells) compared to *wt* (n = 31 cells) [mean soma size *wt* = 110 ± 30 μm², *fh/fh* = 226.5 ± 52 μm²; $F(1,62) = 120.32$, $P < 0.001$]. Therefore, like the reduction in cell number, the increase in cell size occurs before the onset of seizures.

As shown in Figure 4*A–C*, neuronal hypertrophy was not evident in pyramidal cells retrogradely labeled with DiI (Fig. 4*A*), or labeled immunohistochemically using an antibody that recognizes rat brain pyramidal cells (Fig. 4*B*). We compared the soma sizes from *fh/fh* and *wt* pyramidal neurons that contained only single nuclei. As shown in Figure 4*C*, we found that soma sizes of retrogradely labeled pyramidal cells in *wt* (n = 35 cells) are actually slightly larger than pyramidal cells in *fh/fh* (n = 31 cells) [mean *wt* = 241 ± 57 μm², *fh/fh* = 199 ± 41 μm²; $F(1,64) = 11.45$, $P < 0.01$]. Additionally, while the nuclear areas of the same pyramidal neurons show no difference between *fh/fh* (n = 31 cells) and *wt* (n = 35 cells) [*wt* mean = 115 ± 22 μm², *fh/fh* mean = 107 ± 27 μm²; $F(1,64) = 1.858$; $P > 0.05$], nuclei of single-nucleated GABA+ neurons in *fh/fh* (n = 32 cells) are almost twice as large as *wt* (n = 32 cells) [*wt* mean = 93 ± 17 μm², *fh/fh*:

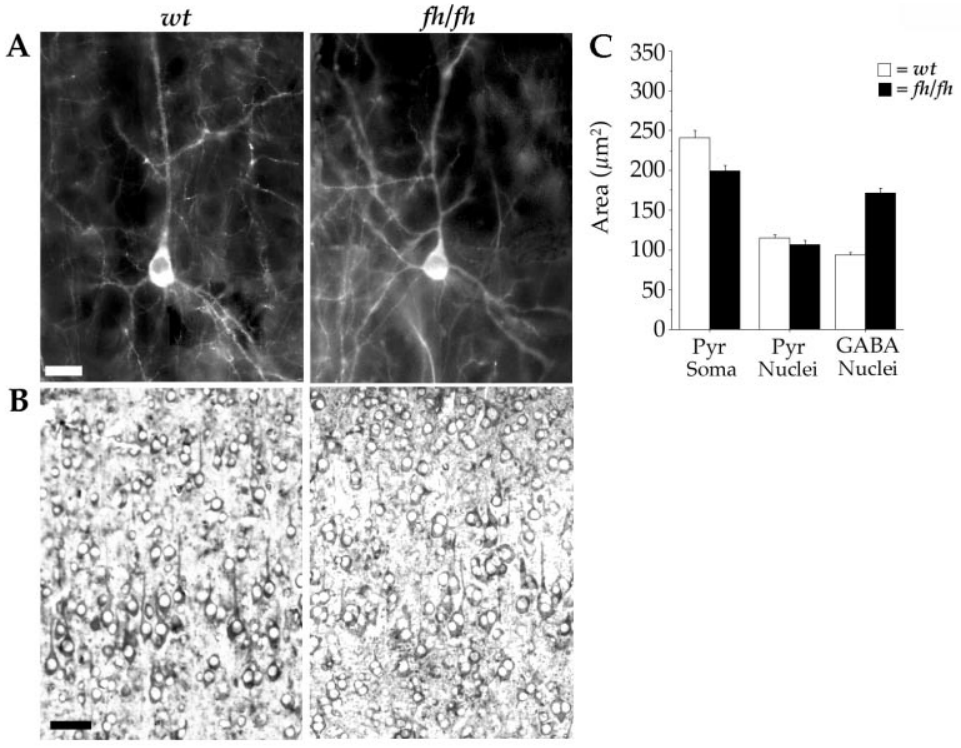

Figure 4. Pyramidal neurons in *fh/fh* do not show similar morphological changes. (*A*) Examples of retrogradely DiI-labeled, upper layer pyramidal neurons in *wt* (left) and *fh/fh* (right) at P15. Cells from both genotypes showed typical prominent apical and basal dendrites. (*B*) Examples of neurons in *wt* (left) and *fh/fh* (right) SS cortex labeled with an anti-rat brain pyramidal cell marker at P16. Pyramidal neurons throughout all layers are similar in size for both genotypes. (*C*) Quantification of soma and nuclear size of DiI-labeled pyramidal cells and nuclear size of GABA-positive cells. On average, *fh/fh* showed significantly smaller pyramidal soma size. In contrast to the nuclei of GABA-positive cells, nuclei of *fh/fh* pyramidal neurons were not different from *wt*. Scale bar (*A*) 25 μm, (*B*) 50 μm.

mean = 171 ± 34 μm^2; $F(1,62) = 134.30$; $P < 0.001$]. Therefore, the *fh* mutation alters cellular growth mechanisms in neocortex specific to interneurons.

Increased Cell Death and Mitotic Abnormalities in the MGE

In order to determine if there are cellular defects within the GE at the time when interneurons are generated, we performed an EM analysis. As shown in Figure 5*A*, an increased number of pyknotic cells are present in the MGE and neocortical VZ in *fh/fh* compared to *wt*. Figure 5*B* shows an electron micrograph of MGE, revealing numerous apoptotic (Fig. 5*B*, left) and multinucleate cells (Fig. 5*B*, right). As shown in Figure 5*C*, the total percentage of pyknotic cells in the MGE at E14 in *fh/fh* compared to *wt* is increased by ~6-fold. Similarly, the total percentage of cell death in *fh/fh* neocortical VZ compared to *wt* is increased by ~3-fold. In addition, *fh/fh* shows a significantly greater number of pyknotic cells in the MGE than in the neocortical VZ[6% compared to 3%; $F(1,10) = 26.28$, $P < 0.001$], and similarly the ratio of pyknotic cells in MGE:VZ is twofold greater in *fh/fh* than in *wt* (2.08 versus 1.03 respectively). Moreover, we observed that the location of many multinucleate cells (Fig. 5*B*, left) in MGE is intermixed and corresponds to the location where cell death is maximal, ~150–300 μm away from the ventricular surface (Fig. 5*D*) and thus appears more concentrated in the SVZ. Therefore, a failure in cytokinesis near the ventricular surface may precede or be closely linked to the cell death in the MGE.

As in the embryo, in P14 neocortex we observed multinucleate non-pyramidal cells (Fig. 6*A*). In additional experiments, we injected BrdU at E14 and at P13 we found many non-pyramidal shaped cells containing two nuclei, both equivalently labeled with BrdU (Fig. 6*B*). In no multinucleate cases was only one nuclei BrdU-labeled. We found that across neocortex in *flathead*, ~27% (257/944) of GABA+ cells contain two nuclei, and ~1% (9/944) contain three or four nuclei, while ~9% (127/1472 cells) of DiI-labeled pyramidal neurons contain two nuclei (Fig. 6*C*) and none contain more than two. Therefore, like MGE, abnormalities in cytokinesis are also found in postnatal neocortex and appear to affect interneurons more so than pyramidal neurons.

Discussion

The *flathead* mutation results in a widespread reduction in the relative number of cortical GABAergic interneurons. At E14, high levels of cell death are observed in both the MGE and neocortical proliferative areas compared to *wt*. This cell death is associated with the appearance of multinucleate cells found in both MGE and throughout postnatal neocortex. The cytokinesis defect appears to affect more non-pyramidal than pyramidal cells in *flathead*, and there is also a selective and specific increase in interneuron growth. Based on these results we hypothesize that the primary defect in *fh/fh* occurs sometime during neurogenesis and that the ensuing cell death in all telencephalic progenitors occurs as a result of failed cytokinetic properties. These observations are consistent with recent data described in Citron-K deficient mice which also have dramatic losses in neocortical interneurons and massive cell death associated with altered cytokinesis (Di Cunto *et al.*, 2000). Since we have recently sequenced and identified a mutation in the Citron-K

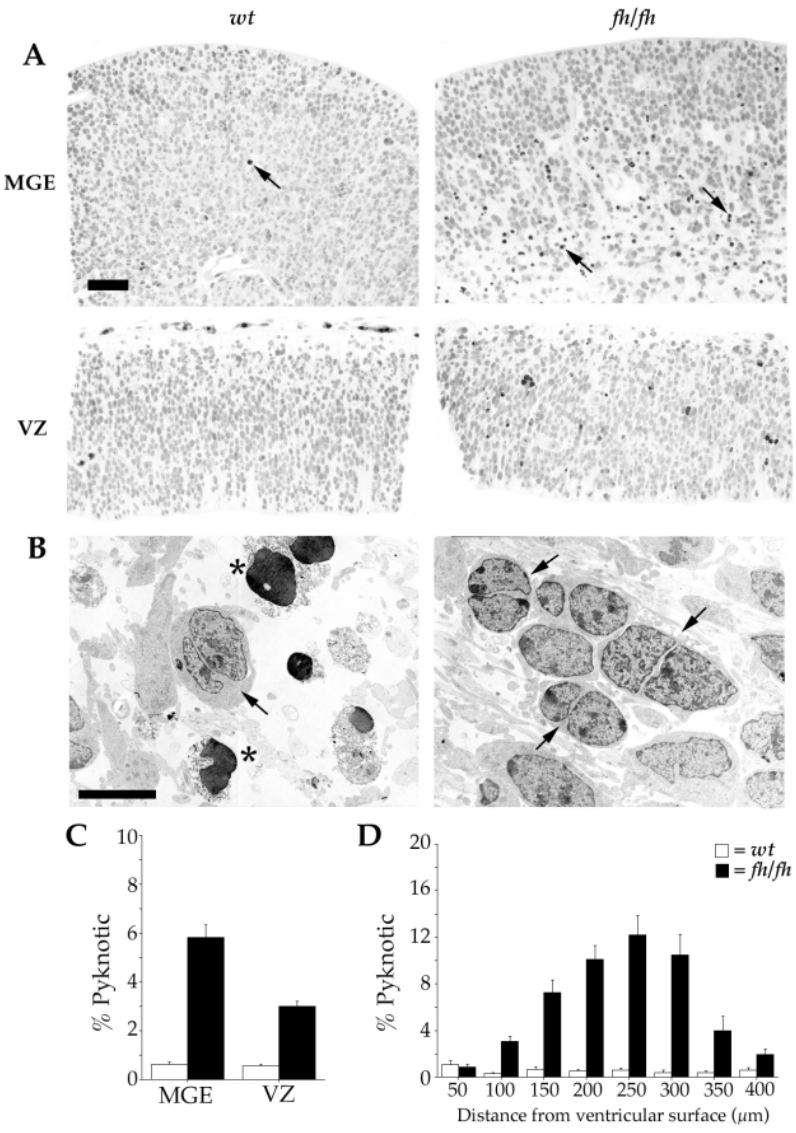

Figure 5. Increased cell death and multinucleate cells in MGE. (*A*) Examples of semi-thin sections of MGE and neocortical-VZ taken in *wt* (left panels) and *fh/fh* (right panels) stained with toluidine blue. For both MGE and neocortical VZ, increased numbers of pyknotic nuclei (arrows) can be observed in *fh/fh*. (*B*) Representative EM of *fh/fh* MGE showing apoptotic cells (asterisks, left panel) and also multinucleate cells (arrows, left and right panels). (*C*) Quantitative analysis of the percentage of pyknotic cells in MGE and neocortical VZ in *wt* (open bars) and *fh/fh* (closed bars). *Flathead* has significantly more cell death in MGE and neocortical VZ compared to *wt*, and there is significantly more cell death in MGE compared to neocortical VZ in *fh/fh*. (*D*) The location of apoptotic cells in MGE relative to the MGE ventricular surface in *fh/fh*. Most apoptotic cells are found 150–300 μm away from the ventricular surface. Scale bar (*A*) 100 μm; (*B*) 5 μm.

gene in *flathead* (unpublished data), it is likely that similar mechanisms of cell death are occurring in *flathead* as the Citron-K deficient mouse. Citron-K is expressed throughout CNS progenitor regions, so it is unclear at this time why the size and number of neocortical interneurons in *flathead* are more severely affected. The overall neocortical phenotype of the *flathead* mutant, however, would indicate that the *flathead* gene is critical for the generation of interneurons and later generated neurons such as upper layer pyramidal neurons.

Regulation of Interneuron Growth and Differentiation

Unlike pyramidal neurons, interneurons in *flathead* have larger somas and dendritic arbors than wildtype. One possibility for the interneuron-specific hypertrophy is that interneuron growth may be negatively regulated by interneuron-specific interactions, and that the reduction in interneuron number in *flathead* results in a corresponding compensatory increase in interneuron growth. If so, then areas of reduced interneuron number should show greater hypertrophy and regions of higher interneuron number should show reduced hypertrophy. However, when we made comparisons of sizes of interneurons across different neocortical regions (EC and SS) we found no significant relationship between the density of GABAergic interneurons in a particular cortical area or lamina with the size of interneurons (three-factor ANOVA; $F = 0.446$, $P = 0.64$). Therefore, a reduction in interneuron interactions alone is not the likely cause of the

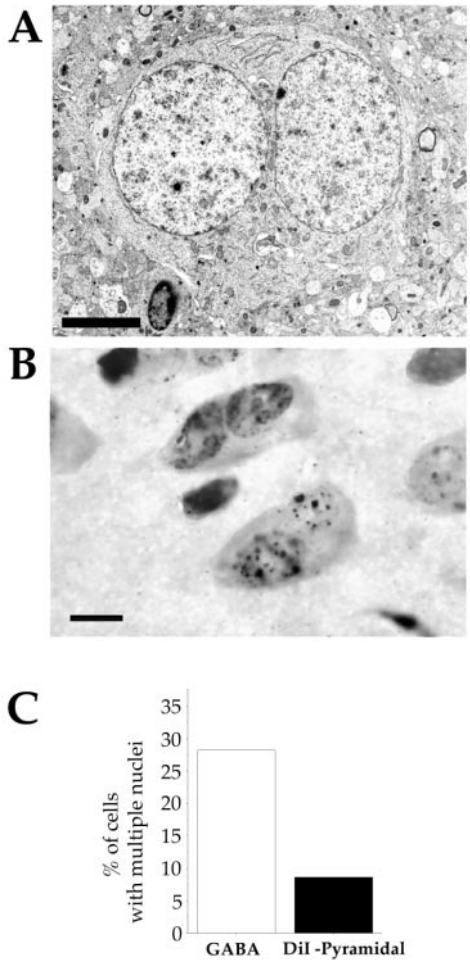

Figure 6. Many non-pyramidal cells in *fh/fh* are multinucleate. (*A*) EM example of a non-pyramidal shaped cell in SS neocortex with two nuclei at P14. (*B*) Examples of two Nissl-stained cells in P13 SS cortex double-labeled for BrdU. BrdU was injected at E14. Note that the cells have two nuclei that are equivalently labeled with BrdU. (*C*) ~28% (266/944 cells) of all GABA+ cells across neocortex compared to ~9% (127/1472 cells) of DiI-labeled, upper layer pyramidal cells are multinucleate. Scale bar (*A*) 5 μm; (*B*) 10 μm.

interneuron-specific hypertrophy; however, there may be a minimum number of interneurons necessary to exert an influence on growth.

Another possibility for the interneuron hypertrophy may be a response to other developmental defects, such as pyramidal neuron cell death in *fh/fh*. For example, interneurons have been previously shown to be very responsive to increases in neurotrophins. Marty *et al*. (Marty *et al*., 1996) found that in hippocampus, brain-derived neurotrophic factor (BDNF), which is not synthesized by interneurons themselves, can increase the size of NPY interneurons, and recent unpublished data indicate that BDNF mRNA levels are increased in the *flathead* neocortex (P. Crino, unpublished observation). Similarly, in BDNF knockout mice, there is a decrease in the number of CAL, PARV and NPY+ cells, and BDNF overexpression increases the number and size of PARV+ cells in neocortex (Jones *et al*., 1994; Huang *et al*., 1999). The increased interneuron growth in *flathead*, which is greater than any previously reported hypertrophy, seems therefore to be the result of an early cell-autonomous increase in cell growth; however, we cannot rule out extrinsic influences at this time. It is not clear why pyramidal neurons with or without double nuclei do not show similar dramatic changes in morphology. However, since multinucleate pyramidal cells do not appear as similarly hypertrophied as multinucleate interneurons may reflect a cell type intrinsic difference in cell growth mechanisms. Further studies in the *fh/fh* brain need to examine the interrelationship between interneurons and pyramidal neurons and whether or not one cell type may be regulating the growth patterns of the other.

Relationship to Human Cortical Dysplasias

Alterations in number, morphology and function of interneurons have been reported in brains of humans with cortical malformations and epilepsy (Ferrer *et al*., 1994; Spreafico *et al*., 1998; Garbelli *et al*., 1999; Hannan *et al*., 1999; Kerfoot *et al*.., 1999) [for review see (DeFelipe, 1999)]. DeFelipe *et al*. (DeFelipe *et al*., 1993) and Marco *et al*. (Marco *et al*., 1996) have reported selective decreases in PARV and glutamic acid decarboxylase immunoreactivity in human epileptogenic neocortex. Spreafico *et al* (Spreafico *et al*., 1998) reported three patients with cortical dysplasias and intractable seizures in which a decrease in PARV, CAL and CR+ cells was observed within the dysplastic regions. In addition, these authors and others (Ferrer *et al*., 1992; Garbelli *et al*., 1999; Thom *et al*., 2000) have reported cytomegalic CAL+ and PARV+ cells, similar in appearance to the cells in *flathead*. Finally, since no other animal model shows similar interneuron hypertrophy along with epileptiform activity, the *flathead* mutant offers a unique opportunity to study the role of cytomegalic interneurons in the generation of seizures.

Cytokinesis Failure and Cell Death in the Flathead Mutant

Our electron microscopy results indicate that many cells just outside of proliferative zones have double nuclei, and binucleate neurons are present in mature postnatal brain as well (Figs 5 and 6). These observations suggest that abnormalities in cell cycle progression in CNS progenitors may underlie the *flathead* phenotype. In particular, the mutation may affect the final phases of cell division which results in failed cytokinesis, and in some cases is followed by cell death. It is difficult to determine whether cytokinesis failure or cell death is most responsible for the decrease in neuron number in the *flathead* mutant; however, there are several reasons why we believe that cytokinesis defects precede the cell death in the *flathead* mutant. First, we have seen BrdU-labeled binucleate cells following BrdU injections as early as E14 (Fig. 6*B*); second, there is no difference in the percentage of S-phase cells in *flathead* proliferative zones (Roberts *et al*., 2000); third, the increased cell death in *flathead* occurs away from the ventricular surface in the same region as the appearance of binucleate precursors (Fig. 5*B*); and fourth, the *flathead* mutation is likely to be in the Citron-K gene, which is a known regulator of cytokinesis (Madaule *et al*., 1998).

The cell death revealed in this study may further explain the resultant cortical phenotype in *fh/fh*. By genotyping E14 embryos with a microsatellite marker <1 cM from the *flathead* gene, before animals are micrencephalic, we determined that there is increased apoptosis in homozygous mutants as early as E14. This not only contrasts the cell death previously reported to begin at E17–18, but it is also greater than that observed at E16 in proliferative zones (Roberts *et al*., 2000). While it is difficult to compare quantitatively cell death determined by TUNEL with that determined by pyknotic nuclei, it is clear that increased cell

death occurs in the proliferative zones of the *flathead* mutant beginning near the time neurogenesis starts, and then increases further towards the end of the neurogenetic period. This could indicate that the mechanisms for cytokinesis control are different in early neurogenesis and in late neurogenesis. Indeed, it has been shown that the pattern of symmetric and asymmetric divisions changes as neocortical neurogenesis proceeds. The pattern of binucleate cells in mature *flathead* cortex may also indicate a greater susceptibility to cell death for cells that must migrate long distances. In *fh/fh* neocortex, we have observed that higher percentages of cells in deeper layers of both EC and SS are multinucleate compared to upper layers (EC: upper = 13%, deeper = 28%, and SS: upper = 11% deeper = 47%). Therefore, one possibility is that longer migrating cells (upper layer neurons from neocortical VZ and interneurons derived from GE–VZ) are at greater risk of dying because double nuclei may not be permissive to longer distance migrations. In fact, we observed a concentration of dead cells in MGE which appear to be within SVZ (Fig. 6*A*) and this death may be associated with a failed attempt to migrate towards neocortex. However, since many of the surviving interneurons in upper and deeper layers of cortex are binucleate, double nuclei must not completely impede all migration.

The Flathead Mutation: Similarities to Citron-K Knockout Mice

Ongoing genetic analysis of the *fh* mutation in our laboratory has lead to two candidate genes located on the distal arm of chromosome 12: Musashi and Citron. Musashi is an RNA binding protein expressed in CNS progenitors (Sakakibara *et al.*, 1996). Citron-K, the embryonic variant of Citron, is expressed specifically in proliferating areas of the CNS and plays a role in cytokinesis (Madaule *et al.*, 1998). Citron-K mutant mice show a striking phenotypic similarity to the *flathead* rat, and we therefore believe it is the most likely candidate for the *flathead* gene (Di Cunto *et al.*, 2000). Mice lacking Citron-K, like the *flathead* mutant rat, show massive apoptosis outside of the VZ surface, early onset and severe seizures, a significant loss of neocortical GABAergic neurons (including dramatic reductions in CAL+ and CR+ subtypes), reduced migration of GABAergic neurons from the GE to neocortex, and altered cytokinesis leading to binucleate pyramidal and nonpyramidal neurons (Di Cunto *et al.*, 2000). We have recently sequenced and identified a mutation in Citron-K in the *fh/fh* mutant (unpublished data). In future reports we will describe the exact molecular mutation and describe how it affects cytokinesis of neocortical pyramidal and nonpyramidal neuronal progenitors.

Notes

We would like to thank Steve Daniels and Dr Marie Cantino at the University of Connecticut Electron Microscopy Facility for their technical assistance in this study. This work was supported by NIH grant MH56524 to J.J.L., A March of Dimes grant 0307 to J.J.L., and, in part, by research grant HD20806, NIH.

Address correspondence to Joseph J. LoTurco, Ph.D., Department of Physiology and Neurobiology, University of Connecticut, U-156, 3107 Horsebarn Hill Road, Storrs, CT 06269, USA. Email: loturco@oracle.pnb.uconn.edu.

References

Alcántara S, de Lecea L, Del Río JA, Ferrer I, Soriano E (1996) Transient colocalization of parvalbumin and calbindin D28k in the postnatal cerebral cortex: evidence for a phenotypic shift in developing nonpyramidal neurons. Eur J Neurosci 8:1329–1339.

Anderson SA, Eisenstat DD, Shi L, Rubenstein JLR (1997) Interneuron migration from basal forebrain to neocortex: dependence on Dlx genes. Science 278: 474–476.

Anderson S, Mione M, Yun K, Rubenstein JLR (1999) Differential origin of neocortical projection and local circuit neurons: role of Dlx genes in neocortical interneuronogenesis. Cereb Cortex 9:646–654.

Anderson SA, Marin O, Horn C, Jennings K, Rubenstein JL (2001) Distinct cortical migrations from the medial and lateral ganglionic eminences. Development 128:353–363.

Benes FM, McSparren J, Bird ED, SanGiovannia JP, Vincent SL (1991) Deficits in small interneurons in prefrontal and cingulate cortices of schizophrenic and schizoaffective patients. Arch Gen Psychiat 48:996–1001.

Cauli B, Audinat E, Lambolez B, Angulo MC, Ropert N, Tsuzuki K, Hestrin S, Rossier J (1997) Molecular and physiological diversity of cortical nonpyramidal cells. J Neurosci 17:3894–3906.

Celio MR (1990) Calbindin D-28k and parvalbumin in the rat nervous system. Neuroscience 35:375–475.

Cogswell CA, Sarkisian MR, Leung V, Patel R, D'Mello SR, LoTurco JJ (1998) A gene essential to brain growth and development maps to the distal arm of rat chromosome 12. Neurosci Lett 25:1–4.

De Carlos JA, López-Mascaraque L,Valverde F (1996) Dynamics of cell migration from the lateral ganglionic eminence in the rat. J Neurosci 16:6146–6156.

DeFelipe J (1997) Types of neurons, synaptic connections and chemical characteristics of cells immunoreactive for calbindin-D28k, parvalbumin and calretinin in the neocortex. J Chem Neuroanat 14:1–19.

DeFelipe J (1999) Chandelier cells and epilepsy. Brain 122:1807–1822.

DeFelipe J, Garcia Sola R, Marco P, del Río MR, Pulido P, Ramón y Cajal S (1993) Selective changes in the microorganization of the human epileptogenic neocortex revealed by parvalbumin immunoreactivity. Cereb Cortex 3:39–48.

Di Cunto F, Imarisio S, Hirsch E, Broccoli V, Bulfone A, Mighelli A, Atzori C, Turco E, Triolo R, Dotto GP, Silengo L, Altruda F (2000) Defective neurogenesis in citron kinase knockout mice by altered cytokinesis and massive apoptosis. Neuron 28:115–127.

Ferrer I, Pineda M, Tallada M, Oliver B, Russi A, Oller L, Noboa R, Zujar MJ, Alcántara S (1992) Abnormal local-circuit neurons in epilepsia partialis continua associated with focal cortical dysplasia. Acta Neuropathol 83:647–652.

Ferrer I, Oliver B, Russi A, Casas R, Rivera, R (1994) Parvalbumin and calbindin-D28k immunocytochemistry in human neocortical epileptic foci. J Neurol Sci 123:18–25.

Garbelli R, Munari C, De Biasi S, Vitellaro-Zuccarello L, Galli C, Bramerio M, Mai R, Battaglia G, Spreafico R (1999) Taylor's cortical dysplasia: a confocal and ultrastructural immunohistochemical study. Brain Pathol 9: 445–461.

Gupta A, Wang Y, Markram H (2000) Organizing principles for a diversity of GABAergic interneurons and synapses in the neocortex. Science 287:273–278.

Hannan AJ, Servotte S, Katsnelson A, Sisodiya S, Blakemoore C, Squier M, Molnar Z (1999) Characterization of nodular heterotopia in children. Brain 122:219–238.

Hendry SH, Schwark HD, Jones EG, Yan J (1987) Numbers and proportions of GABA-immunoreactive neurons in different areas of monkey cerebral cortex. J Neurosci 7:1503–1519.

Huang ZJ, Kirkwood A, Pizzorusso T, Porciatti V, Morales B, Bear MF, Maffei L (1999) BDNF regulates the maturation of inhibition and the critical period of plasticity in mouse visual cortex. Cell 98: 739–755.

Jones KR, Farinas I, Backus C, Reichardt LF (1994) Targeted disruption of the BDNF gene perturbs brain and sensory neuron development but not motor neuron development. Cell 76:989–999.

Kalus P, Senitz D, Beckmann H (1997) Altered distribution of parvalbumin-immunoreactive local circuit neurons in the anterior cingulate cortex of schizophrenic patients. Psychiat Res 75:49–59.

Kawaguchi Y, Kubota Y (1993) Correlation of physiological subgroupings of nonpyramidal cells with parvalbumin- and calbindin D-28k-immunoreactive neurons in layer V of rat frontal cortex. J Neurophysiol 70:387–396.

Kerfoot C, Vinters HV, Mathern GW (1999) Cerebral cortical dysplasia: giant neurons show potential for increased excitation and axonal plasticity. Dev Neurosci 21:260–270.

Lavdas AA, Grigoriou M, Pachnis V, Parnavelas JG (1999) The medial ganglionic eminence gives rise to a population of early neurons in the developing cerebral cortex. J Neurosci 19:7881–7888.

Madaule P, Eda M, Watanabe N, Fujisawa K, Matsuoka T, Bito H, Ishizaki

T, Narumiya S (1998) Role of citron kinase as a target of the small GTPase Rho in cytokinesis. Nature 394:491–494.

Marco P, Sola RG, Pulido P, Alijarde MT, Sanchez A, Ramón y Cajal S (1996) Inhibitory neurons in the human epileptogenic temporal neocortex: an immunocytochemical study. Brain 119: 1327–1347.

Martín-Partido G, Alvarez S, Rodríguez-Gallardo L (1986) Differential staining of dead and dying embryonic cells with a simple new technique. J Microsc 142:101–106.

Marty S, Berninger B, Carroll P, Thoenen H (1996) GABAergic stimulation regulates the phenotype of hippocampal interneurons through the regulation of brain-derived neurotrophic factor. Neuron 16: 565–570.

McCormick DA, Connors BW, Lighthall JW, Prince DA (1985) Comparative electrophysiology of pyramidal and sparsely spiny stellate neurons of the neocortex. J Neurophys 54:782–806.

Meinecke D, Peters A (1987) GABA immunoreactive neurons in rat visual cortex. J Comp Neurol 261:388–404.

Parnavelas JG (2000) The origin and migration of cortical neurones: new vistas. Trends Neurosci 23:126–131.

Parnavelas JG, Lieberman AR, Webster KE (1977) Organization of neurons in the visual cortex, area 17, of the rat. J Anat 124:305–322.

Parnavelas JG, Anderson SA, Lavdas AA, Grigoriou M, Pachnis V, Rubenstein JLR (2000) The contribution of the ganglionic eminence to the neuronal cell types of the cerebral cortex. Novartis Found Symp 228:129–147.

Ribak CE, Bradburne RM, Harris AB (1982) A preferential loss of GABAergic, symmetric synapses in epileptic foci: a quantitative ultrastructural analysis of monkey neocortex. J Neurosci 2:1725–1735.

Roberts MR, Bittman K, Li W, French R, Mitchell B, LoTurco JJ, D'Mello SR (2000). The flathead mutation causes CNS-specific developmental abnormalities and apoptosis. J Neurosci 20:2295–2306.

Sakakibara S, Imai T, Hamaguchi K, Okabe M, Aruga J, Nakajima K, Yasutomi D, Nagata T, Kurihara Y, Uesugi S, Miyata T, Ogawa M, Mikoshiba K, Okano H (1996) Mouse-Musashi-1, a neural RNA-binding protein highly enriched in the mammalian CNS stem cell. Dev Biol 176:230–242.

Sánchez MP, Frassoni C, Álverez-Bolado G, Spreafico R, Fairén A (1992) Distribution of calbindin and parvalbumin in the developing somatosensory cortex and its primordium in the rat: an immunocytochemical study. J Neurocytol 21:717–736.

Sarkisian MR, Rattan S, D'Mello SR, LoTurco JJ (1999) Characterization of seizures in the flathead rat: a new genetic model of epilepsy in early postnatal development. Epilepsia 40:394–400.

Spreafico R, Battaglia G, Arcelli P, Andermann F, Dubeau F, Palmini A, Olivier A, Villemure JG, Tampieri D, Avanzini G, Avoli M (1998) Cortical dysplasia: an immunocytochemical study of three patients. Neurology 50:27–36.

Sussel L, Marin O, Kimura S, Rubenstein JLR (1999) Loss of Nkx2.1 homeobox gene function results in a ventral to dorsal molecular respecification within the basal telencephalon: evidence for a transformation of the pallidum into the striatum. Development 126:3359–3370.

Tamamaki N, Fujimori KE, Takauji R (1997) Origin and route of tangentially migrating neurons in the developing neocortical intermediate zone. J Neurosci 17:8313–23.

Thom M, Holton JL, D'Arrigo C, Griffin B, Beckett A, Sisodiya S, Alexiou D, Sander JW (2000) Microdysgenesis with abnormal cortical myelinated fibres in temporal lobe epilepsy: a histopathological study with calbindin D-28-k immunohistochemistry. Neuropathol Appl Neurobiol 26:251–257.

Wichterle H, Garcia-Verdugo JM, Herrera DG, Alvarez-Buylla A (1999) Young neurons from the medial ganglionic eminence disperse in adult and embryonic brain. Nat Neurosci 2:461–466

Wouterlood FG, Härtig W, Brückner G, Witter MP (1995) Parvalbumin-immunoreactive neurons in the entorhinal cortex of the rat: localization, morphology, connectivity and ultrastructure. J Neurocytol 24: 135–153.